

Vacuum Brazing Studies on High Manganese Stainless Steel

Differences in behavior of 19 brazing filler metals on a relatively new austenitic stainless steel and on type 304 are established

BY W. S. BENNETT, R. F. HILLYER,
D. L. KELLER AND D. H. RIEFENBERG

ABSTRACT. Vacuum brazing studies have been conducted on a relatively new austenitic stainless steel of nominal composition 21Cr-6Ni-9Mn-0.3N. Wettability tests using 19 commercial brazing filler metals have been run over wide brazing temperature ranges on this steel and on type 304 for comparison. These results are reported as wetting index versus temperature for each steel and each brazing filler metal alloy. The nature and extent of interaction between the brazing alloys and the steels has been analyzed by conventional metallography and electron microprobe analysis. The individual reactions are described in some detail. The reactions are similar for both steels except for copper or gold-copper brazing filler metals. These brazing alloys penetrate into the high manganese steel to a much greater extent than on 304 and are probably not acceptable for most applications of this material.

Introduction

In the past few years a new austenitic stainless steel has come into

use. This alloy, referred to here as high manganese stainless steel, HMSS, has a nominal room temperature yield strength of 65,000 psi (44.8 megapascals). The corrosion resistance of this alloy equals or exceeds that of 304 stainless steel in most environments. The alloy has proven quite useful at cryogenic temperatures due to its very stable austenite. The composition of the alloy is given in Table 1. The high yield strength is due primarily to solid solution strengthening by nitrogen. The high chromium content accounts for the excellent corrosion resistance while the manganese and nitrogen produce the very stable austenitic structure.

Using high energy rate forging (HERF) techniques, the yield strength can be raised to 120,000 psi (82.8 megapascals) while at the same time maintaining elongations of over 30%. The HERF structure is thermally stable for short periods of time to approximately 825 C.

In certain applications the alloy must be brazed in the HERF condition; thus brazing filler metals must be available which produce adequate flow and wetting at brazing temperatures below 825 C. Other applications use the alloy in the annealed condition so the temperature restriction is not applicable and higher temperature braze metals are of interest. In all of our applications, extreme

cleanliness is necessary so all brazing is done without flux and in vacuum.

Considerable information was available on vacuum brazing 300 series stainless steels. In early attempts to use this information on HMSS some differences in brazing alloy flow and base metal reaction were noted. It was then decided to undertake a study of wettability and base metal reaction of 19 commercial braze metals on HMSS and compare this behavior with that of 304L stainless steel. The majority of the alloys were based on the silver-copper eutectic with various elements added to enhance wettability. Other alloys used were gold, silver, or copper base alloys. The majority of the alloys had been used successfully on 300 stainless steels. The chemistry and the liquidus, solidus, and brazing temperatures are given in Table 2.

Experimental Procedures

Wettability specimens, 2 in. (50.8 mm) diam by $\frac{1}{8}$ in. (3.17 mm) thick were prepared from HMSS and 304 bar stock. A $\frac{1}{16}$ in. (1.58 mm) diam by $\frac{1}{2}$ in. (12.2 mm) deep thermocouple hole was drilled at the edge of each specimen. The specimens were thoroughly degreased in acetone and polished on 400 grit metallographic paper. The samples were then de-

The authors are associated with Dow Chemical Company, Rocky Flats Division, Golden, Colorado.

Paper was presented at the 55th AWS Annual Meeting (Fifth International AWS-WRC Brazing Conference) held at Houston, Texas, during May 7-9, 1974.

greased again. Braze metal samples were also thoroughly degreased in acetone. All braze metals were in wire form of 0.020 in. (0.51 mm) or 0.025 in. (0.63 mm) diam wire. The wire was formed into coils of approximately 1/8 in. (3.17 mm) O.D. Total volume of braze metal used was 0.008 cm³ (0.00005 in.³).

The stainless steel samples with the braze metal on the sample were placed in a standard, cold wall vacuum furnace. Chromel-Alumel thermocouples were inserted into each sample. The furnace was evacuated to 5 × 10⁻⁶ torr or lower. The samples were heated to the selected brazing temperature and held for 5 min. The samples were then cooled by flowing helium to at least 150 C before removing them from the furnace. The area of braze metal flow and the contact angle were then measured.

Transverse cross sections through the center of the braze metals were mounted and prepared metallographically. The microstructures were examined optically at several magnifications. The cross sections were then analyzed with x-ray microprobe analysis. Elemental maps of each major alloying element in the steels and each element in the braze metals were made for each cross section (Ref. 1). These maps are an optical read out of the intensity of the characteristic x-radiation produced when the sample is bombarded with a 20 kV electron beam. This type of map allows qualitative analyses of the various phases present. By careful counting techniques, quantitative analyses can be done, but such analyses are very time consuming. Quantitative analysis was done on only a few selected samples.

Figure 1 shows a typical elemental map with a braze interface aligned through the center of the figure. This particular map shows the distribution of nickel in the cross section. The map shows a uniform concentration of nickel in the steel, a heavy concentration of nickel at the interface, and almost no nickel in the braze metal. These maps, plus the optical metallography allow analyses of the braze metal-base metal interactions.

Results and Discussion

The contact angle and braze metal flow measurements for each steel at several temperatures represents a large amount of data and in tabular form is not very readable. To condense the amount of data, a wetting index as developed by Feduska (Ref. 2) has been used. The wetting index (W. I.) equals the area covered by the braze metal times the cosine of the contact angle. The W. I. for each braze metal has been plotted versus

temperature and these are shown in Fig. 2 through 16. Note that the W. I. here cannot be compared directly with those of Feduska because of differences in the amount of braze metal used. The W. I. of this study varied from 0, where no wetting occurred, to a maximum of 0.27. In our tests, W. I. values of 0.05 are considered good

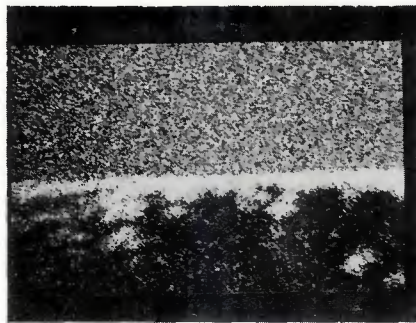


Fig. 1—Example of elemental map for nickel; concentration of nickel in any area is proportional to number of white dots in the area

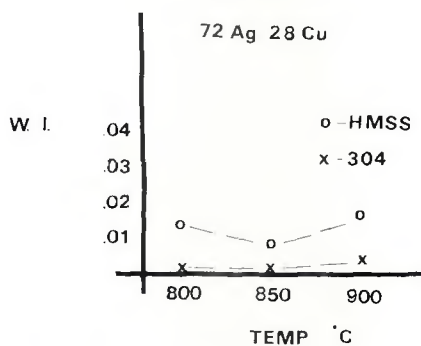


Fig. 2—W. I. vs. Temperature, alloy no. 5

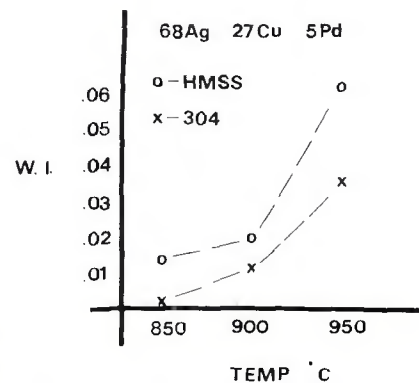


Fig. 3—W. I. vs. Temperature, alloy no. 6

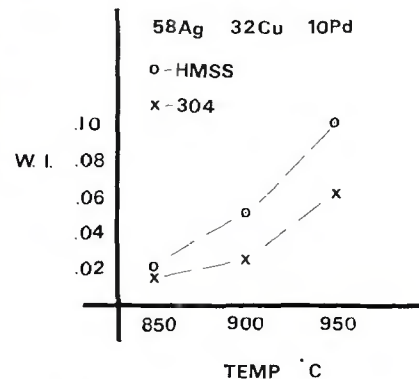


Fig. 4—W. I. vs. Temperature, alloy no. 7

Table 1 — Composition of High Manganese Stainless Steel

| Element | wt% |
|-------------|-------------|
| Chromium | 18.0 - 21.0 |
| Nickel | 5.5 - 7.5 |
| Manganese | 8.0 - 10.0 |
| Silicon | 1.0 Max |
| Nitrogen | 0.15 - 0.40 |
| Phosphorous | 0.060 Max. |
| Carbon | 0.040 Max. |
| Sulfur | 0.030 Max. |

Table 2 — Brazing Filler Metal Alloys Studied

| Filler metal no. | Composition, wt% | Liquidus temp C | Solidus temp C | Brazing temperatures studied, C |
|------------------|--------------------|-----------------|----------------|---------------------------------|
| 1 | 62Ag-24Cu-15In | 705 | 630 | 750, 800, 850 |
| 2 | 63Ag-27Cu-10In | 730 | 685 | 750, 800, 850 |
| 3 BAg-8a | 71.8Ag-28Cu-0.2Li | 760 | 760 | 800, 850, 900 |
| 4 BAg-19 | 92.5Ag-7.3Cu-0.2Li | 890 | 760 | 950, 1000, 1050 |
| 5 BAg-8 | 72Ag-28Cu | 780 | 780 | 800, 850, 900 |
| 6 | 68Ag-27Cu-5Pd | 810 | 807 | 850, 900, 950 |
| 7 | 58Ag-32Cu-10Pd | 852 | 824 | 850, 900, 950 |
| 8 | 65Ag-20Cu-15Pd | 900 | 850 | 900, 950, 1000 |
| 9 | 54Ag-21Cu-25Pd | 950 | 900 | 950, 1000 |
| 10 | 71.5Ag-28Cu-0.5Ni | 795 | 780 | 800, 850, 900 |
| 11 | 63Ag-28Cu-6Sn-3Ni | 800 | 690 | 800, 850 |
| 12 | 65Ag-28Cu-5Mn-2Ni | 850 | 750 | 850, 900 |
| 13 BAg-18 | 60Ag-30Cu-10Sn | 720 | 600 | 750, 800, 850 |
| 14 | 57Ag-33Cu-7Sn-3Mn | 730 | 605 | 750, 800, 850 |
| 15 BAu-4 | 82Au-18Ni | 950 | 950 | 950, 1000 |
| 16 | 60Au-20Ag-20Cu | 845 | 830 | 850, 900, 950, 1000 |
| 17 | 81.5Au-16Cu-2.5Ni | 925 | 910 | 950, 1000, 1050 |
| 18 | 85Cu-7Ag-8Sn | 985 | 665 | 100, 1050 |
| 19 BAg-Mn | 85Ag-15Mn | 970 | 960 | 1000, 1050, 1100 |

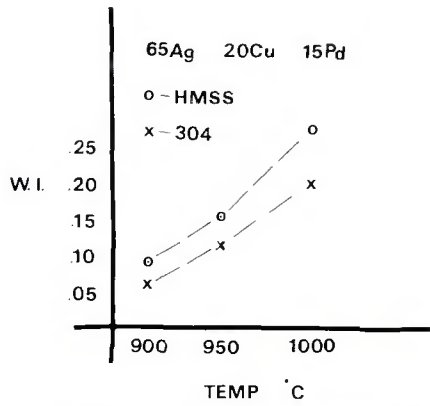


Fig. 5—W. I. vs. Temperature, alloy no. 8

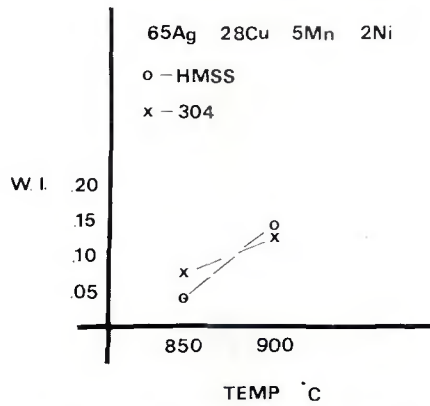


Fig. 9—W. I. vs. Temperature, alloy no. 12

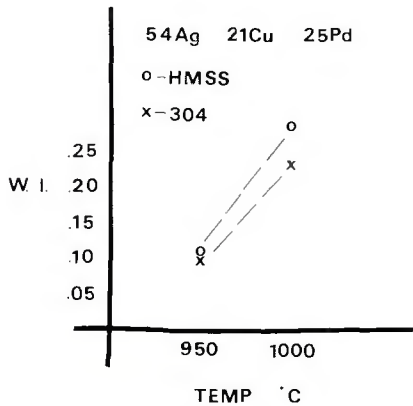


Fig. 6—W. I. vs. Temperature, alloy no. 9

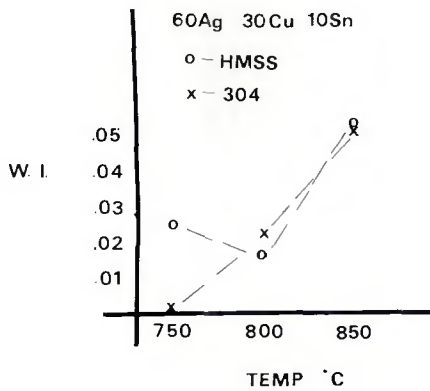


Fig. 10—W. I. vs. Temperature, alloy no. 13

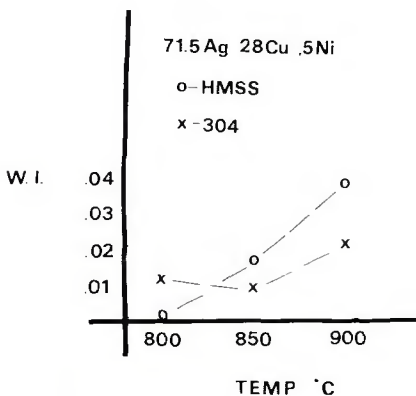


Fig. 7—W. I. vs. Temperature, alloy no. 10

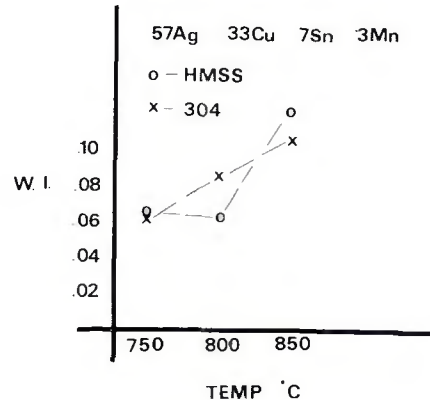


Fig. 11—W. I. vs. Temperature, alloy no. 14

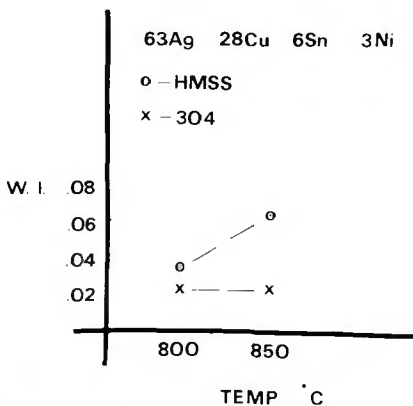


Fig. 8—W. I. vs. Temperature, alloy no. 11

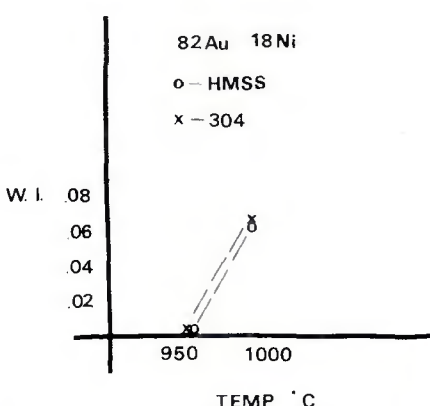


Fig. 12—W. I. vs. Temperature, alloy no. 15

wettability and values of 0.10 are considered excellent. In reviewing Fig. 2 through 16 note that the increments for W. I. vary from figure to figure. The variation was necessary to keep the figures as compact as possible.

Four of the alloys tested (numbers 1 through 4) produced no wetting on either 304 or HMSS. These materials were silver-copper alloys with lithium or indium additions. Lithium additions to silver base brazing filler metals used in hydrogen are reported to enhance wetting (Ref. 3). The enhancement is thought to be due to deoxidation of the base metal surface by the lithium.

In our studies on brazing alloys containing lithium, a dull film formed around the brazing alloy droplet. This film, apparently due to lithium reacting with the steel surface, appeared to completely inhibit wetting. The surface reaction seems to be modified by the high vacuum environment, making such alloys unsuited to vacuum brazing. Indium additions lower the melting point of the silver-copper eutectic and are reported to increase wetting on ferrous alloys in hydrogen, inert gas, or vacuum atmospheres (Ref. 4). It was expected that wetting and flow would occur at temperatures well below 825 C. In our studies no wetting occurred at brazing temperatures up to 850 C. No explanation is offered for the differences in behavior.

The wettability of the silver-copper eutectic is shown in Fig. 2. Essentially, no wetting occurs on 304 and only minimal wetting on HMSS. This was expected as this alloy is not recommended for use on ferrous alloys (Ref. 5). Additions of other alloying elements were quite effective in enhancing wetting. Wettability results for silver-copper-palladium alloys are shown in Figs. 3 through 6. The wettability increases with increasing palladium content. The 15 wt% and 25 wt% palladium alloys showed the maximum W. I. of any of the alloys used in this study. All four alloys had better wettability on HMSS than on 304. None of the alloys produced good wetting below 900 C.

Nickel is a common element added to silver-copper alloys to enhance wettability. Figure 7 gives the results of adding 0.5 wt% nickel to the silver-copper eutectic. Some improvement occurs but wetting is only marginal. Figure 8 shows the effect of nickel plus tin additions. This alloy produces good wetting on HMSS at 850 C but only marginal wetting on 304. Nickel plus manganese seems to be more effective as shown in Fig. 9. Fair to good wetting occurs at 850 C and excellent wetting occurs at 900 C. A silver-copper-tin alloy is shown in Fig. 10. This alloy produces

some wetting on HMSS at 750 C. However, it is necessary to raise the temperature to 850 C before good wetting is achieved. Tin plus manganese additions combine to produce the most effective alloy in the lower temperature range as shown in Fig. 11. This alloy produces good wetting at 750 C. This was the only alloy studied which produced good flow on HMSS at temperatures low enough to prevent any loss of mechanical properties in the HERF condition.

Three gold alloys are shown in Figs. 12 to 14. The gold-nickel alloy, Fig. 12, is a widely used alloy for brazing stainless steels. It does show good wetting on both steels at 1000 C. A lower melting gold alloy is shown in Fig. 13, but it is still necessary to heat to 1000 C before much wetting occurs. Figure 14 shows the wettability of a gold-copper-nickel alloy. This alloy flows much more readily on HMSS than on 304.

Figures 15 and 16 show the results for two miscellaneous alloys. The copper alloy in Fig. 15 produces excellent wetting on both steels. The silver manganese alloy shown in Fig. 16 has frequently been used for stainless steel brazing. It does produce some wetting and the amount of wetting shows little change with temperature indicating little interaction with the base metal.

The metallographically prepared cross sections and the microprobe elemental maps have been combined into single figures. Using Fig. 17 as an example, a 200X cross section of the brazing alloy-base metal interface is shown for both HMSS and 304. The compositions of the individual phases in the brazing alloy and reaction zone are identified by lines drawn to a typical region of each phase. The elemental make-up of each phase is then given by the elements listed for that line. The elements in each phase are listed in order of decreasing concentration, as can best be judged from the elemental maps. Since these maps are only qualitative, some of the listed orders could easily be out of sequence. The brazing temperatures of the cross sections shown are generally near the top of the temperature ranges investigated.

Figure 17 shows a typical interface for all of the silver-copper-palladium alloys. The braze metal away from the interface consists of two phases, a silver phase, a dark colored phase, and a copper-palladium phase, the light colored phase. At the interface a continuous layer of the copper-palladium phase has formed. Iron has dissolved into this phase, and in some of the cross sections, islands of copper-palladium-iron have formed in the brazing alloy up to 0.003 in. (0.076

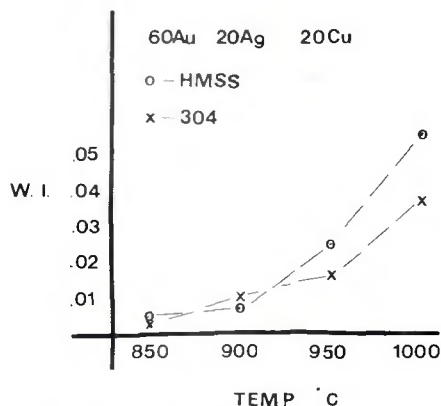


Fig. 13—W. I. vs. Temperature, alloy no. 16

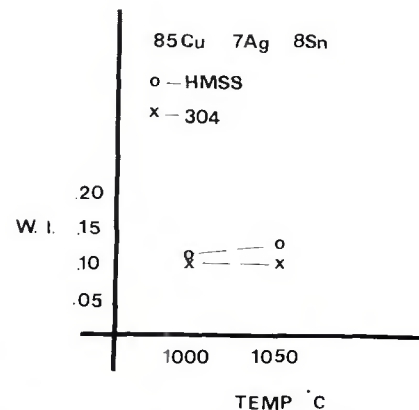


Fig. 15—W. I. vs. Temperature, alloy no. 18

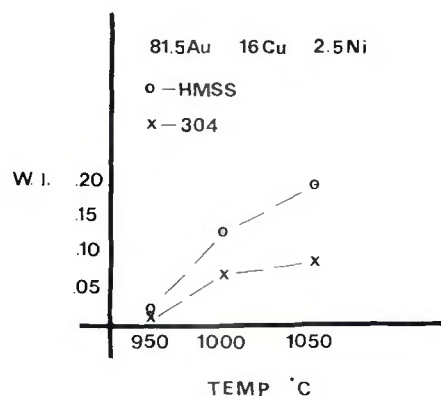


Fig. 14—W. I. vs. Temperature, alloy no. 17

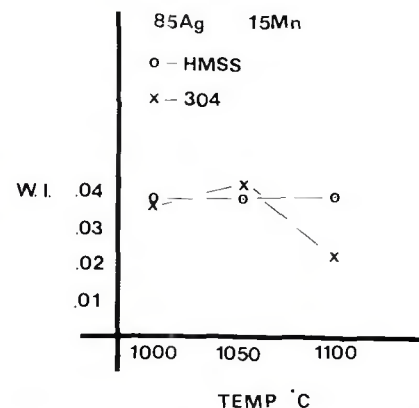


Fig. 16—W. I. vs. Temperature, alloy no. 19

mm) from the interface. In the 15 wt% and 25 wt% palladium alloys at the higher temperatures, the interface reactions become somewhat more severe, especially on the HMSS alloy. Some chromium, nickel and manganese dissolve into the copper-palladium layer. Very little, if any, penetration of braze metal into the base metal occurs. This series of alloys seems to be well suited to brazing austenitic stainless steels in the 900 to 1000 C temperature range because of its excellent wetting characteristics and moderate erosion rates.

Silver-copper alloys containing nickel additions have exhibited an unusual distribution of elements at the interface. Figure 18 shows the cross sections for silver-copper eutectic alloy, number 10, containing 0.5 wt% nickel. The major portion of the braze metal is a eutectic mixture of silver and copper. At the interface a continuous layer of copper-nickel has formed. No nickel can be seen anywhere else in the braze. It appears that all the nickel in the braze metal is concentrated in this surface layer. Further, it appears that the nickel comes only from the braze metal and not from the steel because the nickel layer forms only when the braze metal

contains nickel. A small amount of iron is dissolved into the nickel-copper layer. No penetration of braze metal into the steel can be seen. The reactions seem to be identical on both steels.

Figure 19 shows another silver-copper alloy containing nickel and manganese, alloy 12. The light colored phase is silver. The dark phase contains copper and manganese. No nickel is detectable in either phase. Again, a continuous layer has formed at the interface. Here this layer contains copper, nickel and some increased concentration of manganese compared to the bulk of the braze metal. No iron or chromium has dissolved into this layer and no penetration of braze metal into the steels has occurred. It is surprising that the reactions between the steels and the braze metal are no more severe than this in view of the excellent wetting behavior of this alloy.

Figure 20 shows alloy 11, a third silver-copper alloy containing additions of nickel and tin. The structure of this alloy is very much the same as alloys 10 and 12; a silver phase, a copper phase containing tin and a copper-nickel layer at the interface. Again, no nickel is detected in the

bulk of the braze. Some iron has dissolved into this nickel layer, very similar to alloy 10. Again the reaction on each steel is nearly identical.

The formation of a nickel rich interface layer in silver-copper-nickel alloys is well known and is credited

with preventing interface corrosion in stainless steel braze joints made with these alloys (Ref. 6). What was surprising was the degree of concentration of the nickel at the interface. Further, when manganese is present in this layer, as in alloy 12, dissolu-

tion of the base metal is reduced and wetting is enhanced. When tin is present in the alloy the wetting and reaction are much the same as when only nickel is present.

When tin alone is present in the silver-copper alloy as in alloy 13, no in-

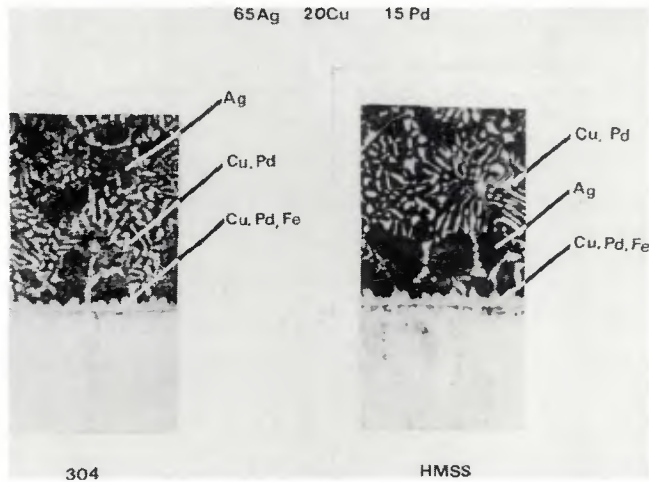


Fig. 17—Cross section of alloy no. 8 at 900 C

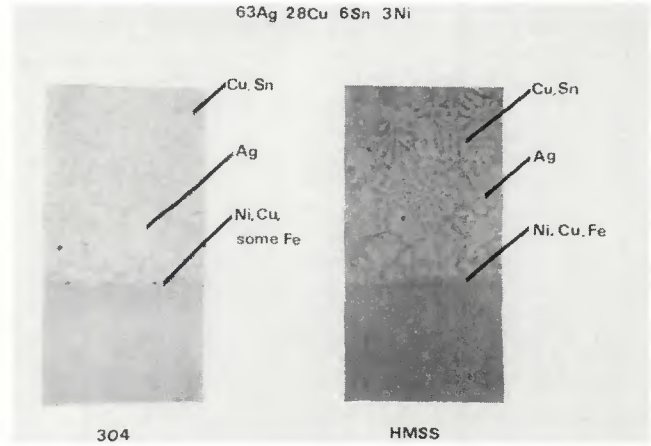


Fig. 20—Cross section of alloy no. 11 at 850 C

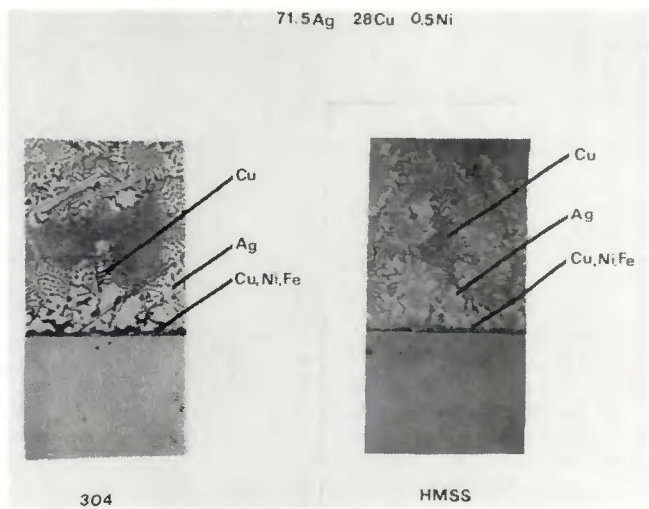


Fig. 18—Cross section of alloy no. 10 at 900 C

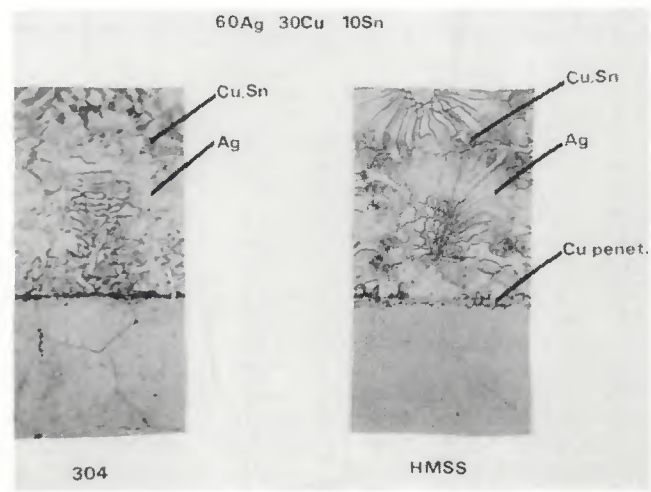


Fig. 21—Cross section of alloy no. 13 at 800 C

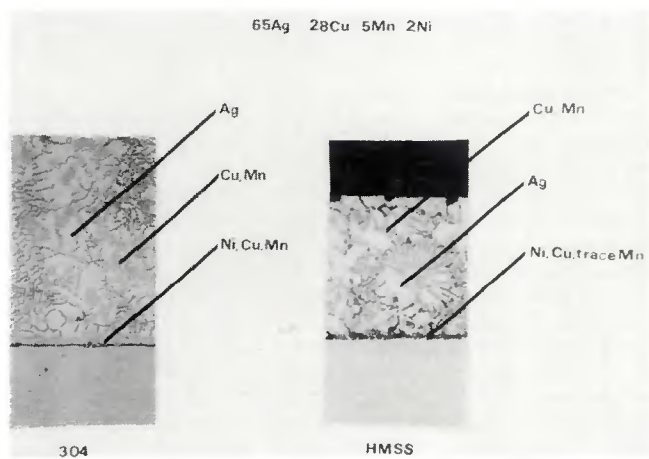


Fig. 19—Cross section of alloy no. 12 at 900 C

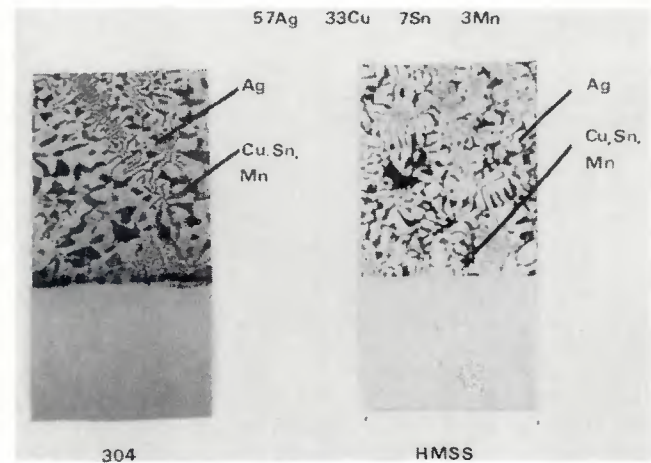


Fig. 22—Cross section of alloy no. 14 at 800 C

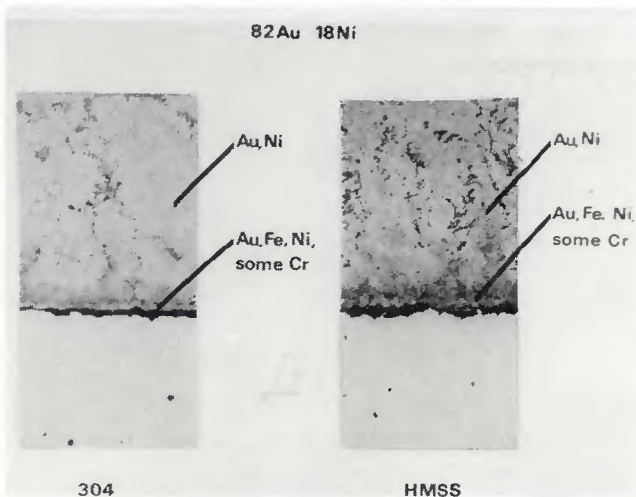


Fig. 23—Cross section of alloy no. 15 at 1000 C

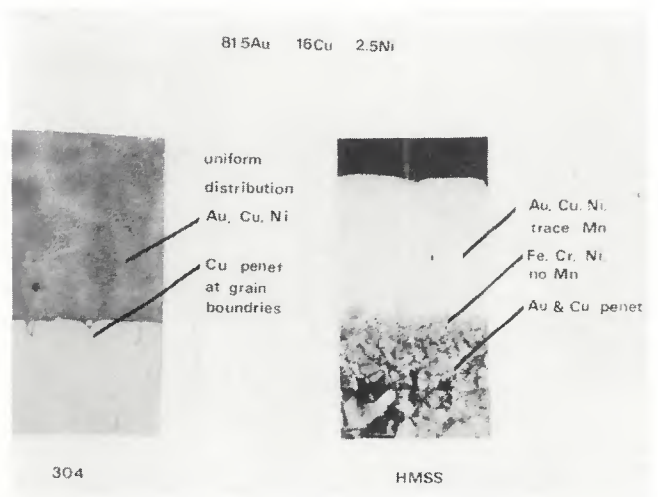


Fig. 24—Cross section of alloy no. 17 at 1000 C

terface layer forms at all. The cross sections of this alloy are shown in Fig. 21. The braze metal consists of two phases, a silver phase and a copper-tin phase. The tin clearly increases wettability as shown in the wetting studies but causes no interface layers to form as palladium and nickel do. Some slight copper penetration into the steel, to a depth of 0.0002 in. (0.005 mm) has occurred on the HMSS. No further reactions can be seen.

Alloy 14 contains both tin and manganese additions and cross sections of these interfaces are shown in Fig. 22. Again a silver phase is present and a copper-tin-manganese phase. No interface layers are present, no dissolution of the steels can be seen and no penetration of braze metal into the steel can be seen. Alloying of braze metal with the steel takes place on such a limited scale that it cannot be detected with the elemental maps. The combination of manganese and tin greatly enhances the wetting and at the same time holds reaction to a minimum. On the basis of wettability and interaction this alloy seems to be nearly ideal for use on austenitic stainless steels.

Figure 23 gives the metallographic results of alloy 15, a gold-nickel alloy. The etching response of the bulk braze metal would indicate two phases present. This is apparently an artifact of the etching process. The microprobe maps show a uniform distribution of gold and nickel, as would be expected from the phase relationship for this alloy. The interface of both steels shows as much as 0.001 in. (0.0254 mm) variation in height due to local dissolution of the steel into the braze metal. Iron is detectable a few thousandths of an inch into the braze metal. Erosion of the base metal might become a problem with this alloy if an unusually long or high

temperature braze cycle were used, but no problems should be encountered in normal braze cycles.

Figure 24 gives the cross sections for a gold-copper-nickel alloy, number 17. The W. I. is much higher on HMSS than it is on 304. As the cross sections show, the reaction between the two steels and the brazing alloy is much different. On 304, the bulk braze metal consists of a uniform distribution of gold, copper and nickel. No interface layers can be detected but copper penetration of the steel grain boundaries occurs to a depth of about 0.001 in. (0.025 mm). On HMSS the braze metal reacts much more with the steel. The braze metal has penetrated the base metal to a depth of about 0.003 in. (0.076 mm). Both copper and gold can be detected at this depth. Entire grains of steel have been loosened and are dispersed into the bulk brazing alloy. In the region where penetration has occurred, no manganese is detectable in the steel. Small amounts of manganese are now dissolved into the bulk alloy. It appears that the manganese in the affected region has moved entirely from the steel into the filler metal.

Alloy 16, a gold-copper-silver alloy is shown in Fig. 25. The reactions with this alloy are much the same as the preceding one. The bulk braze consists of two phases, a gold-copper phase and a gold-copper-silver phase. Braze metal penetration of the grain boundaries in 304 has again occurred to a depth of 0.0015 in. (0.038 mm). On HMSS the braze metal has penetrated to about 0.003 in. (0.076 mm) and has again loosened grains from the steel and these grains are displaced up into the brazing alloy. Again, these grains are free of manganese and there is manganese depletion in the area where the braze metal has penetrated. Manganese was not detected in the braze metal in

this alloy.

Figure 26 shows alloy 18, a copper-tin-silver alloy. The brazing alloy consists of large grains of copper with some tin and spaced between these grains a second phase of tin and silver. On 304, copper has penetrated the base metal to a depth of about 0.0002 in. (0.005 mm). The interface layer shown in the cross section is apparently composed of steel grains with copper penetration in between. No other change in composition can be seen on the elemental maps. On HMSS the copper penetration is much greater, up to 0.004 in. (0.10 mm). But here, the grains of steel are not displaced from the interface. Further, there is no manganese depletion in the penetration areas as occurred with the gold-copper alloys.

The reactions between HMSS and copper or gold-copper brazing alloys are clearly far more severe than on the 300 series stainless steels. The increase in severity is apparently due to interaction between copper and manganese. At brazing temperatures, copper and manganese are completely soluble and produce a minimum in the liquidus curve at 870 C. It appears that manganese very easily dissolves into copper allowing the copper to penetrate and erode the steel. The presence of gold in the alloy seems to accelerate the dissolution of manganese. The reasons for such an increase are not clear.

One other alloy has been studied, alloy 19, a silver-manganese alloy shown in Fig. 27. The bulk braze metal consists of a single phase solution of manganese in silver. Very little reaction occurs between the braze metal and the base metal on either steel. A slight roughening of the interface has occurred on 304 but no dissolution of one material into the other can be seen on the elemental maps.

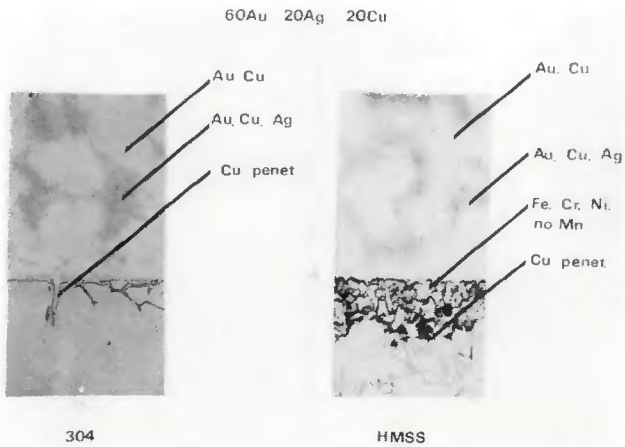


Fig. 25—Cross section of alloy no. 16 at 1000 C

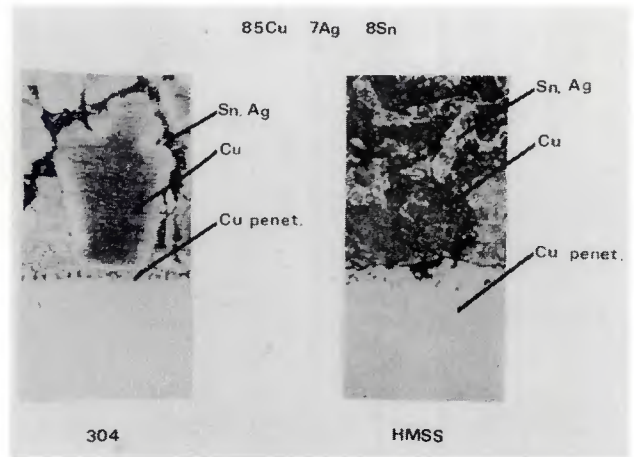


Fig. 26—Cross section of alloy no. 18 at 1000 C

Due to the high brazing temperatures and only fair wetting, this alloy does not seem particularly desirable for these steels. However, the nearly total lack of interaction during brazing might indicate its use in special situations.

Conclusions

1. Silver-copper eutectic-type alloys with 10 or 15 wt% indium additions produced no wetting on either 304 or HMSS at temperatures up to 850 C and vacuum level of 5×10^{-5} torr.

2. Silver-copper alloys with lithium additions did not produce any wetting on either 304 or HMSS. This is also in contrast to reported behavior in hydrogen atmospheres. The high vacuum apparently modifies the surface reactions of lithium.

3. The degree of wetting of most braze alloys on HMSS was equal to or better than on 304.

4. Only one alloy, 57Ag-33Cu-7Sn-3Mn, produced satisfactory wetting on HMSS at low enough temperatures to prevent thermal change in the HERF structures. Further, this alloy showed a minimum reaction with the base metal making it a very desirable braze alloy for austenitic stainless steels.

5. The extent of reaction between the silver-copper eutectic type alloys and both 304 and HMSS was minimal. Both steels produced about the same amount of reaction and in no case did the degree of reaction appear to be sufficient to prohibit use of any of the alloys.

6. Reaction between copper or copper-gold and 304 results in some grain boundary penetration. Generally, this penetration is not sufficient to exclude their use on 304. The degree of reaction of these brazing alloys on HMSS is markedly in-

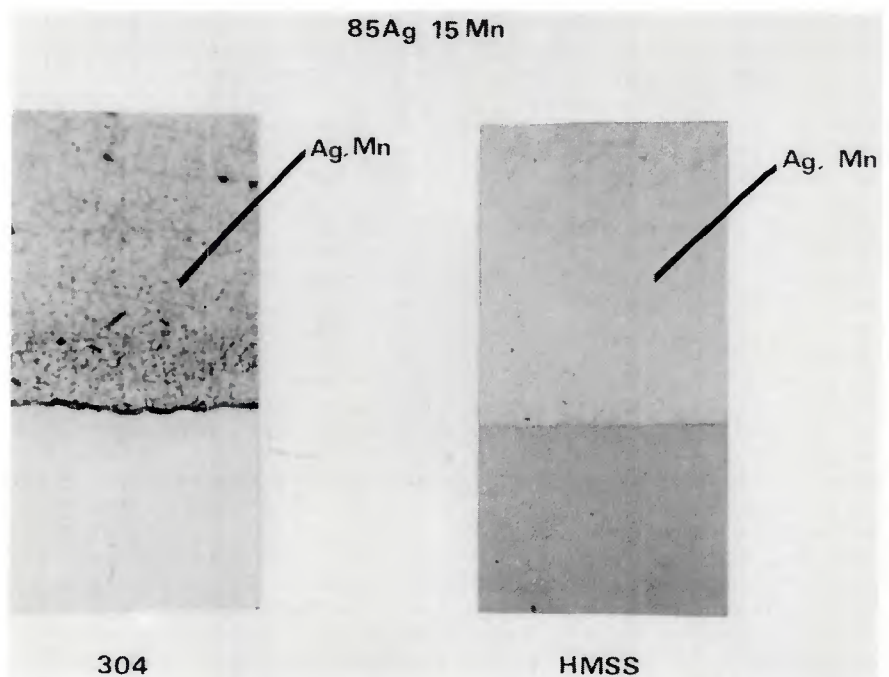


Fig. 27—Cross section of alloy no. 19 at 1050 C

creased compared with 304. The braze metals penetrate several thousandths of an inch into the steel and separate some grains of steel from the base metal. Further, in the penetrated region, the steel is completely depleted of manganese apparently due to the solubility of manganese in copper. The interactions are severe enough to forbid the use of these braze alloys in most applications of HMSS.

References

1. Riefenberg, D. H., Doyle, J. H., Hill-
 yer, R. F., Bennett, W. S., "Characteriza-

tion of Brazing Alloys," RFP 2233, Dow
 Chemical, U.S.A., To be published.

2. Feduska, W., "High Temperature
 Brazing Alloy-Base Metal Wetting Re-
 actions," *Welding Journal*, Vol. 38, (3),
 March 1959. Res. Suppl., pp 122-s to
 130-s.

3. McDonald, A. S., "Alloys for Brazing
 Thin Sections of Stainless Steel," *Welding
 Journal*, Vol. 36, (3), March 1957, Res.
 Suppl., pp 131-s to 140-s.

4. Handy and Harman Brazing Data
 Sheet D-37.

5. Lawless, J. J., "How to Select Brazing
 Alloys," *Machine Design*, 1964.

6. Sistare, G. H., Halbig, J. J., Grenell,
 L. H., "Silver Brazing Alloys for Corrosion-
 Resistant Joints in Stainless Steel," *Weld-
 ing Journal*, Vol. 34, (1), January, 1954, pp
 137-143.